AGU PUBLICATIONS

Geophysical Research Letters

RESEARCH LETTER
10.1002/2017GL074998

Key Points:
- A distinctive echo pattern was found in the LRS data obtained around the Marius Hills Hole (MHH), a possible skylight of a lava tube
- Around an area (13.00–15.00°N, 301.85–304.01°E) around MHH, similar LRS echo patterns were found at several locations
- The locations exhibiting the echo pattern are consistent with mass deficits suggested by the GRAIL gravity data analysis

Supporting Information:
- Supporting Information S1

Correspondence to:
T. Kaku,
7bemm027@mail.u-tokai.ac.jp

Citation:
Kaku, T., Haruyama, J., Miyake, W., Kumamoto, A., Ishiyama, K., Nishibori, T., … Howell, K. C. (2017). Detection of intact lava tubes at Marius Hills on the Moon by SELENE (Kaguya) lunar radar sounder. *Geophysical Research Letters*, *44*, 10,155–10,161. https://doi.org/10.1002/2017GL074998

Received 18 JUL 2017
Accepted 24 SEP 2017
Accepted article online 17 OCT 2017
Published online 25 OCT 2017

Detection of Intact Lava Tubes at Marius Hills on the Moon by SELENE (Kaguya) Lunar Radar Sounder

T. Kaku[1,2], J. Haruyama[1], W. Miyake[2], A. Kumamoto[3], K. Ishiyama[1], T. Nishibori[1], K. Yamamoto[4], Sarah T. Crites[1], T. Michikami[5], Y. Yokota[1,6], R. Sood[7], H. J. Melosh[8,9], L. Chappaz[10], and K. C. Howell[8]

[1]Institute of Space and Astronautical Science, Japan Aerospace Exploration Agency, Sagamihara, Japan, [2]Department of Mechanical Engineering, Graduate School of Engineering, Tokai University, Hiratsuka, Japan, [3]Department of Geophysics, Graduate School of Science, Tohoku University, Sendai, Japan, [4]National Astronomical Observatory of Japan, Sendai, Japan, [5]Faculty of Engineering, Kindai University, Osaka, Japan, [6]Faculty of Science, Kochi University, Kochi, Japan, [7]Department of Aerospace Engineering and Mechanics, College of Engineering, The University of Alabama, Tuscaloosa, AL, USA, [8]School of Aeronautics and Astronautics, Purdue University, West Lafayette, IN, USA, [9]Department of Earth, Atmospheric, and Planetary Science, Purdue University, West Lafayette, IN, USA, [10]AstroLabs, Pasadena, CA, USA

Abstract Intact lunar lava tubes offer a pristine environment to conduct scientific examination of the Moon's composition and potentially serve as secure shelters for humans and instruments. We investigated the SELENE Lunar Radar Sounder (LRS) data at locations close to the Marius Hills Hole (MHH), a skylight potentially leading to an intact lava tube, and found a distinctive echo pattern exhibiting a precipitous decrease in echo power, subsequently followed by a large second echo peak that may be evidence for the existence of a lava tube. The search area was further expanded to 13.00–15.00°N, 301.85–304.01°E around the MHH, and similar LRS echo patterns were observed at several locations. Most of the locations are in regions of underground mass deficit suggested by GRAIL gravity data analysis. Some of the observed echo patterns are along rille *A*, where the MHH was discovered, or on the southwest underground extension of the rille.

1. Introduction

Lunar lava tubes are important from various science perspectives and provide potential sites for future lunar base construction (Coombs & Hawke, 1992; Haruyama et al., 2012; Hörz, 1985; Oberbeck et al., 1969). Since the insides of lava tubes are shielded from meteorite bombardment, cosmic radiation, or particle implantation, they are expected to be in pristine condition, an environment with preserved lava composition, textures, and even volatiles. Careful examination of the interior can add insight concerning the evolutionary history of the Moon. The radiation and meteorite bombardment that disturbs the geologic record at the surface of the Moon also makes it a harsh place for humans and instruments; thus, the inside of an intact lava tube would be the safest place on the Moon from an exploration perspective. Coombs and Hawke (1992) investigated lunar surface segments associated with rilles to infer the existence of intact lava tubes under the surface. However, the Lunar Orbiter and Apollo photographs they used were not conclusive because the image coverage by the photographs was limited and most were nadir observations. No plausible evidence for the existence of intact lava tubes on the Moon was reported in the 20th century.

In 2009, a large, deep hole was discovered in the lunar Marius Hills in image data acquired by the Selenological and Engineering Explorer for SELENE Terrain Camera (TC) with 10 m/pixel resolution from an orbit 100 km above the lunar surface (Haruyama et al., 2009). Both diameter and depth are 50 m (Haruyama et al., 2012, 2016; Robinson et al., 2012). The Marius Hills Hole (MHH) is located in rille *A*, which was once proposed as a primary investigation station for Apollo (Elston & Willingham, 1969; Greeley, 1971; Karlstrom et al., 1968). Haruyama et al. (2009) hypothesized that the hole was a skylight that appeared to be an opening into a lava tube.

Later, higher resolution nadir and oblique angle observations performed by the Lunar Reconnaissance Orbiter Narrow Angle Camera with 50 cm/pixel resolution from an orbit 50 km above the lunar surface confirmed that the MHH is a skylight opening into a large space (Robinson et al., 2012; Wagner & Robinson, 2014); the floor of the hole extended at least several meters eastward and westward under a ceiling of two other

holes, Mare Tranquillitatis Hole and Mare Ingenii Hole (Haruyama et al., 2010). The height from the floor to the ceiling exceeds 15 m for MHH. However, because oblique observations do not penetrate far beneath the rim of the hole, the full extent of the subsurface space around the MHH remained unknown.

Gravity measurements provide one probe to explore the distribution of subsurface structures (Andrews-Hanna et al., 2013; Bills & Ferrari, 1977; Bratt et al., 1985; Thurber & Solomon, 1978; Yamamoto et al., 2016). The existence of a lava tube extending a few to several tens of kilometers in length would affect gravity conditions and be detectable as a "mass deficit." The twin Gravity Recovery and Interior Laboratory (GRAIL) spacecraft were launched in 2011 (Zuber, Smith, Lehman, et al., 2013; Zuber, Smith, Watkins, et al., 2013). The GRAIL representation of the Moon's gravity field is a spherical harmonic expansion, currently reported to degree and order 1,200 (Chappaz et al., 2017). Developing methods of gradiometry and cross correlation to isolate the target signal of mass deficits from the GRAIL gravity data, Chappaz et al. (2017) detected several locations of horizontally extended mass deficits. A lava tube extending a few to several tens of kilometers would be a large enough void to create a mass deficit detectable in the GRAIL data. A mass deficit signature follows rille *A* and is far larger than expected from the topographic trough alone, which implies the existence of a large void space beneath the visible surface extending 60 km to the west of the MHH. Some of the mass deficits detected by Chappaz et al. (2017) could be caused by long open lava tubes (Chappaz et al., 2017). Geologically plausible alternative sources of cave include large highly fractured faults or partially collapsed lava tubes.

Another method to explore the subsurface structure uses ground-penetrating radar systems (e.g., Miyamoto et al., 2005; Phillips et al., 1973; Seu et al., 2004; Seu et al., 2007). Campbell et al. (2009) investigated the Marius Hills using Earth-based radar with 12.6 cm and 70 cm wavelengths and characterized domes by the high circular polarization ratios of the radar data. The 12.6 cm radar signals penetrate up to a meter or two, and the 70 cm data reach about a factor of 5 times greater depth. However, the radar data were not appropriate to detect features deeper than a few tens of meters.

The Lunar Radar Sounder (LRS), an active radar sounder, was installed on SELENE. The operation frequency of the LRS is 4–6 MHz (around 60 m wavelength), and transmission power is 800 W. Subsurface structures at depths of a few hundred meters to a few kilometers have been investigated using LRS data (e.g., Ono et al., 2009; Oshigami et al., 2012; Oshigami et al., 2014). However, most previous works focused on the structure of laterally extensive it. In the present study, we examine in detail the LRS echo data reflected from a few tens of meters to a few hundred meters' depth to confirm the existence of underlying intact lava tubes.

2. Methods

We used radar echo data from the LRS onboard SELENE to investigate the existence of underground lava tubes at depths of a few tens to a few hundreds of meters. The LRS consists of two sets of dipole antennas with a tip-to-tip length of 30 m transmitting electromagnetic (EM) waves and receiving echoes from the Moon or natural radio waves from the Earth and other planets (e.g., Jupiter). The LRS actively transmits frequency-modulated continuous EM waves sweeping from 4 to 6 MHz (around 60 m wavelength) in 200 μs to the Moon. The bandwidth of 2 MHz leads to the range resolution of 75 m in vacuum (dielectric constant ε is 1) and a smaller resolution in the ground depending on the dielectric constant. The transmission interval of LRS is 50 ms, which corresponds to 75 m on the ground in the SELENE flight direction (Kobayashi et al., 2012; Ono et al., 2009). The LRS transmission power of 800 W is designed to detect subsurface boundaries even at depths of a few kilometers. The echoes of EM waves transmitted by LRS antennas are observed with different time delays corresponding to the distances to reflectors, such as surface crater walls and/or subsurface boundaries. The observed LRS echo data are composed of reflections from the surface and subsurface boundaries. We used LRS echo data that were processed using the Synthetic Aperture Radar (SAR) algorithm (Kobayashi et al., 2012). As a result of SAR processing, the signal is limited to returns from the surface and subsurface due east-west of the subspacecraft point. The synthetic aperture size for the LRS echo data used is 5 km. The data set we used is the Sounder SAR image (power) processed using a synthetic aperture of 5 km and is archived in the SELENE Data Archive website (http://l2db.selene.darts.isas.jaxa.jp/index.html.en).

Figure 1 plots a typical LRS echo power data profile in a mare region (13.715°N, 304.010°E). The time differences of received echoes were converted to corresponding depths where the LRS transmitted EM waves

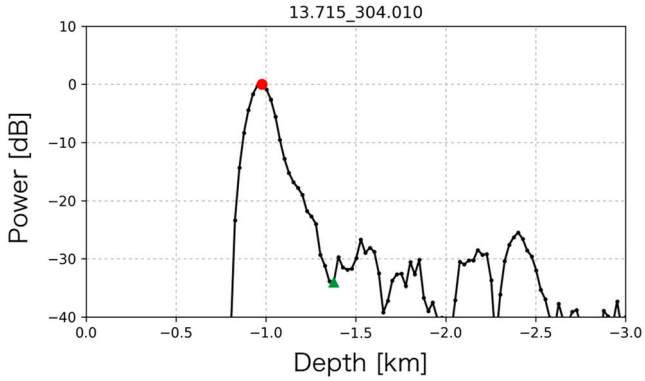

Figure 1. Typical LRS echo power versus subsurface depth. The LRS data were observed at a mare region (13.715°N, 304.010°E). The dielectric constant used here for converting time to depth is unity (1), as if it were a vacuum. The largest echo peak (red point; normalized to 0 dB) is from the nadir surface of the Moon, and subsequently observed echoes gradually decrease in power to the noise level of 34 dB (green triangle), weaker than the noise level of about 25 dB.

transmitted by the LRS were reflected. The dielectric constant used here for converting time-to-depth is unity (1), for vacuum. The true location of the reflectors is therefore shallower than tentatively given with the vacuum dielectric constant value. The largest echo peak (red point; normalized to 0 dB) is from the nadir surface of the Moon. After the largest echo peak, the observed signal level gradually decreases due to adsorption and scattering of EM waves in the underground and finally falls to a noise level of −34 dB (green triangle), weaker than the noise level of about −25 dB.

3. Results

We first investigated the LRS data from a SELENE orbit approaching the MHH (14.100°N, 303.262°E) and found an echo pattern with two peaks at location T1, which is 1.2 km east and 0.3 km south from the MHH. Figure 2 plots the LRS echo power as observed at location T1 versus the subsurface depth from where the LRS radar power was reflected. Here we set the dielectric constant (ε) to that of vacuum, which is 1, to calculate an upper limit for the depth. The first echo peak (red point; normalized to 0 dB) is from the surface, and the second peak (blue square) must be from the subsurface boundary. Prior to the second echo peak, the received echo power decreased precipitously with time to a noise level of −28.1 dB (green triangle). After the second echo peak, the received echo power decreased (orange pentagon). The purple diamond marks the third echo peak. In Figure 2, the depth of the green triangle is 125 m and that of the blue square is 250 m. When we assume a dielectric constant of 4 or higher, a more appropriate value for lunar subsurface materials (Ono et al., 2009), we obtain a more realistic depth of 62.5 m or shallower for the green triangle and 125 m or shallower for the blue square. The subsurface boundary detected at T1 (blue square) may be a ceiling or a floor of a cave, such as an underlying lava tube.

We expanded the search area to 13.00–15.00°N, 301.85–304.01°E around the MHH, in an effort to identify locations with subsurface caves where the echo patterns exhibit the following three characteristic features similar to those of location T1:

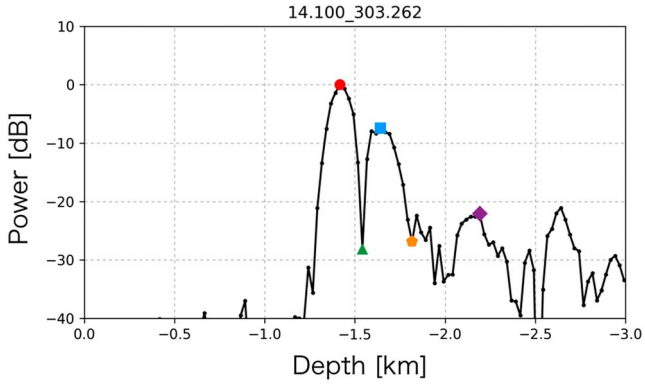

Figure 2. The LRS echo power versus the subsurface depth at location T1 (14.100°N, 303.262°E). The LRS data have an echo pattern with two peaks at T1 1.2 km east and 0.3 km south of the MHH. The dielectric constant used for converting time to depth is unity (1), appropriate for vacuum. The first echo peak (red point; normalized to 0 dB) is from the surface, and the second one (blue square) must be from a subsurface boundary. Prior to the second echo peak, the received echo power precipitously decreased with time to a noise level of −28.1 dB (green triangle). This echo pattern with two peaks and a substantial echo decrease between them implies the existence of a cave, such as an underlying lava tube (see text). After the second echo peak, the received echo power decreased (orange pentagon). The purple diamond marks the third echo peak.

1. The echo power returned from the subsurface regions shallower than 125 m decreases more than 25 dB compared to the surface echo power level (i.e., in Figure 2, echo power of the red point-echo power of the green triangle >25 dB), which indicates the existence of a cave or a homogeneous rock bulge where no change of dielectric constant in the subsurface region occurs, and thus, there is no reflection of sounding EM waves.
2. There is a second echo peak (for example, the blue square in Figure 2) at a depth of less than 225 m from the surface, as observed at location T1, which indicates the existence of a boundary with a change of dielectric constant such as the ceiling or the floor surface of a lava tube.
3. The echo level of the third largest peak (for example, the purple diamond in Figure 2) is smaller than that of the second peak; here we assume that the third echo peak should be weaker than the second one, and any strong third echo should be regarded as that from an off-nadir surface point.

Figure 3 presents the results that mark various locations corresponding to the three aforementioned characteristic features in the vicinity of the MHH. The background of the figure is an image from the SELENE TC. The gray lines correspond to the LRS observation tracks. The circular points on these lines indicate locations where echo patterns satisfy the

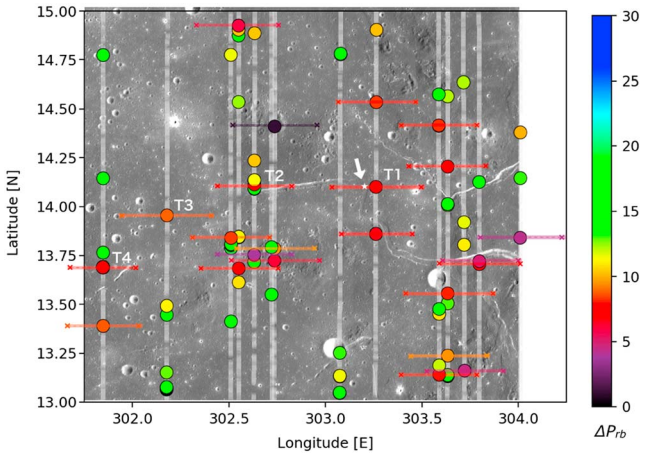

Figure 3. The search led to the identification of locations where LRS echo patterns satisfy the condition of three characteristic features associated with location T1. The background image is from the SELENE TC. The gray lines correspond to the LRS measurement tracks. The color of the circular points denotes the power difference between the first and the second echo peaks (ΔPrb). The bars around the candidate sites indicate equidistances corresponding to portions where reflectors yielding the second echo peaks should exist. The half of widths of bars around T1 are 6.990 km. As a result of SAR processing, echoes from subsurface boundaries, and/or echoes from reflectors at due east or due west off-nadir surface remain (X marks on the bars). The location of the MHH (a white star) is indicated by an arrow.

condition of the three characteristic features possibly suggesting a cave, based on the echo pattern determined at location T1. More than 80 locations, candidate sites of possible subsurface caves, were detected in this search area. The colors of the circles denote the power difference between the first and second echo peaks (ΔPrb: a point indicated by a red circle-a point by a blue square in Figure 2). Some candidate sites for the presence of a cave exhibit strong second echo peaks; the lower the ΔPrb value, the more likely the presence of a subsurface lava tube (for instance, at circle points with black to red colors in Figure 3). Some of the candidate cave sites are aligned along rille *A* (T2) and on a possible extension of rille *A* (T3 and T4). The location of the MHH (a white star in Figure 3) is indicated by an arrow.

4. Discussion

We found several candidate sites for intact lava tube caves where a large second peak of radar echo transmitted by the SELENE LRS was observed with an interval characterized by a precipitous decrease in echo power after the largest echo from the nadir surface. Some of the candidate sites were at rille *A*, where a skylight hole of a possible subsurface lava tube had been discovered (Haruyama et al., 2009).

There are two interpretations of the echo pattern with two peaks and a substantial echo decrease between them. The first interpretation is that the second echo peak is from the ceiling (β boundary) or the floor (γ boundary) of a lava tube, and the echo from the floor of the lava tube was buried in the peak of echo from the ceiling; thus, no additional echo is seen. The decrease in echo power before the second echo peak demonstrates the existence of a large dense rock layer through which the radar passed without any significant reflections. The lava tube must be located deeper than 75 m from the surface, and the height (from floor to ceiling) of the lava tube must be smaller than 75 m. The second interpretation is that the second echo peak is from the floor (γ boundary) of a lava tube, whereas the echo from the ceiling (β boundary) of the lava tube was buried in the peak of echo from the surface. The decrease in echo power before the second echo peak means the existence of a cave through which the radar passed without any reflections. The cave must be located deeper than 75 m, and the height of the lava tube must exceed 75 m. It seems more plausible that the second echo peaks of the candidate sites are from floors, because the precipitous decrease in echo power prior to the second echo peak is most consistent with the presence of vacuum space. Dielectric constants of any lava forming the ceiling of a lava tube would be less homogeneous than that of vacuum space; vacuum space yields a more considerable decrease in echoes (Figure 4).

We investigated whether or not nearby geologic features, such as walls of large craters, may have produced off-nadir EM surface reflectors. Bars were centered on locations where prominent second echo peaks are observed to see if other features may correspond to the second echo. The bars are presented in Figure 3. The half of widths of these bars are 6.990 km around T1, 5.850 km around T2, 6.993 km around T3, and 5.640 km around T4. We used the data for which SAR processing (Kobayashi et al., 2012) was performed. Therefore, besides the surface echo, only echoes from subsurface boundaries and/or from the due east and/or due west surface should remain. The possible locations of the off-nadir surface reflectors with $\Delta\text{Prb} < 10$ dB are marked with X on the bars in Figure 3. However, no topographic feature (e.g., crater walls) that could cause a large off-nadir surface echo has been found at the locations indicated by X marks. Thus, the second echo peaks observed are probably from subsurface boundaries, not from any EM wave reflectors on the surface.

For the same search region (13.00–15.00°N, 301.85–304.01°E around the MHH), we compared the result of Chappaz et al. (2017) based on the twin GRAIL spacecraft data. Figure 5 indicates the lava tube candidate sites as suggested by the LRS data overlaid on a cross-correlation Bouguer gravity map Chappaz et al. (2017) developed. The cold colors on the map are consistent with mass surplus, whereas the hot colors correspond to mass deficits (i.e., low-density space or voids such as caves). Most lava tube candidate sites suggested by

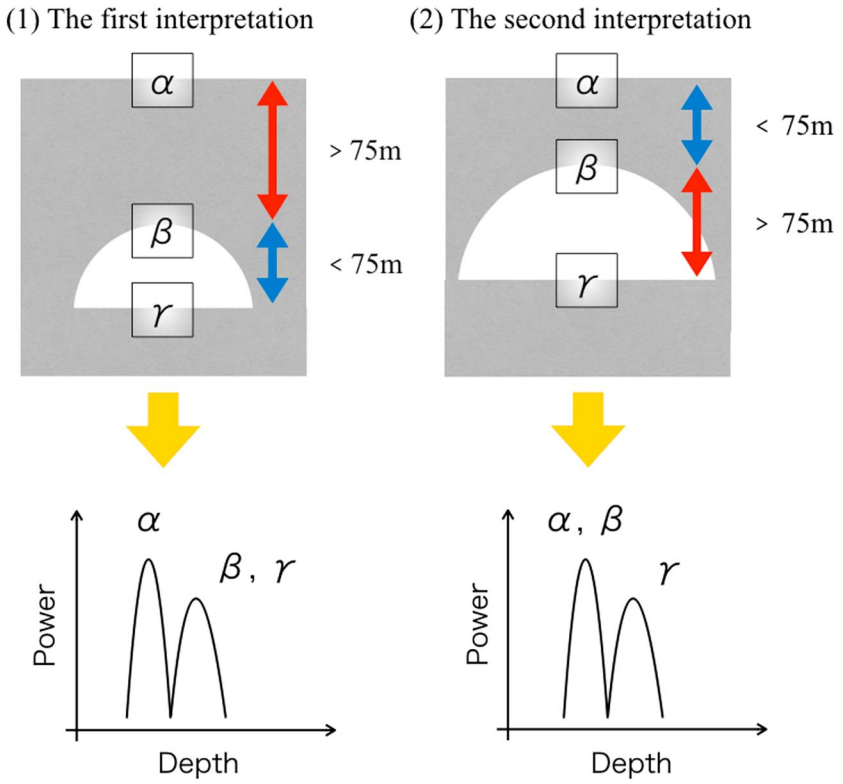

Figure 4. Two interpretations of the echo pattern in LRS data at location T1 (14.100°N, 303.262°E). The first interpretation is that the second echo peak is from the ceiling (β boundary) and the floor (γ boundary) of a lava tube. The decrease in echo power demonstrates the existence of a large dense rock layer. The lava tube must be located deeper than 75 m from the surface, and the height (from floor to ceiling) of the lava tube must be smaller than 75 m. The second interpretation is that the second echo peak is from the floor (γ boundary) of a lava tube, whereas the echo from the ceiling (β boundary) of the lava tube was buried in the peak of echo from the surface. The decrease in echo power before the second echo peak means the existence of a cave. The cave must be located shallower than 75 m, and the height of the lava tube must exceed 75 m.

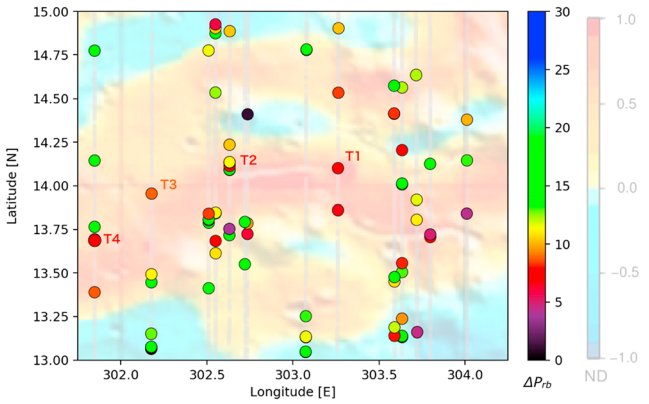

Figure 5. The search identified locations where LRS echo patterns satisfy the condition of three characteristic features associated with T1 and overlaid them on a cross-correlation Bouguer gravity map Chappaz et al. (2017) developed. The cold colors on the map are consistent with mass surplus; the hot colors correspond to mass deficits (i.e., low density space or voids such as caves). Prominent mass deficits are observed on rille *A* and on an extension southwest of the rille (red). Most other lava tube candidate sites not on rille *A* are also in the Bouguer mass deficits (red to yellow).

LRS data are also apparent as LRS data correlate with the area of mass deficits (red to yellow regions) in the cross-correlation Bouguer gravity map. Prominent mass deficits are seen on rille *A* and on an extension to the southwest of the rille (red regions). Therefore, the lava flows that formed rille A may have flowed toward the southwest beyond the visible end of the rille through a tube or roofed over channel.

Some candidate sites are in areas of mass surplus. The circular points of these sites are indicated by green to blue, and the radar echo peak levels for the sites are small. Therefore, the sites may not have any large caves under the subsurface, or they may contain some voids surrounded by a large mass surplus. We note that an area in 13.5–13.8°N, 302.5–302.8°E contains many candidate sites, some of which are SELENE LRS data with a large second echo peak (indicate by red points). Many lava tubes or cavernous voids likely exist below the surface in this region.

5. Conclusions

We investigated the LRS data to detect subsurface intact lava tubes. We found a characteristic feature in LRS data indicating a large

second echo peak after a precipitous decrease in echo close to the MHH, a possible skylight of an underground lava tube. Several locations around the MHH (13.00–15.00°N, 301.85–304.01°E) exhibit similar characteristic features in the LRS data. Since there are no possible features on the surface that could cause a second echo peak, these locations are candidate sites for the presence of underground lava tubes or cavernous voids. We note that most of these candidate sites are at locations consistent with a mass deficit on the cross-correlation Bouguer anomaly map based on GRAIL data. In particular, some lava tube candidate sites are along rille *A*, in which the MHH was discovered, and on a possible underground extension southwest of the rille where the cross-correlation Bouguer map indicates a large mass deficit. In conclusion, we have identified an intact lava tube at Marius Hills on the Moon in SELENE LRS data.

Acknowledgments

This work is supported by JSPS KAKENHI grant 26400459 (JH). H.J.M. was supported by NASA's GRAIL mission. The authors thank W. B. Garry and L. Kestay for their comments, which led to significant improvements in the manuscript.

References

Andrews-Hanna, J. C., Asmar, S. W., Head, J. W. III, Kiefer, W. S., Konopliv, A. S., Lemoine, F. G., … Zuber, M. T. (2013). Ancient igneous intrusions and early expansion of the Moon revealed by GRAIL gravity gradiometry. *Science*, *339*, 675–678. https://doi.org/10.1126/science.1231753

Bills, B. G., & Ferrari, A. J. (1977). A lunar density model consistent with topographic, gravitational, librational, and seismic data. *Journal of Geophysical Research*, *82*, 1306–1314. https://doi.org/10.1029/JB082i008p01306

Bratt, S. R., Solomon, S. C., Head, J. W., & Thurber, C. F. (1985). The deep structure of lunar basins: Implications for basin formation and modification. *Journal of Geophysical Research*, *90*, 3049–3064. https://doi.org/10.1029/JB090iB04p03049

Campbell, B. A., Hawke, B. R., & Campbell, D. B. (2009). Surface morphology of domes in the Marius Hills and Mons Rümker regions of the Moon from Earth-based radar data. *Journal of Geophysical Research*, *114*, E01001. https://doi.org/10.1029/2008JE003253

Chappaz, L., Sood, R., Melosh, H. J., Howell, K. C., Blair, D. M., Milbury, C., & Zuber, M. T. (2017). Evidence of large empty lava tubes on the Moon using GRAIL gravity. *Geophysical Research Letters*, *44*, 105–112. https://doi.org/10.1002/2016GL071588

Coombs, C. R., & Hawke, B. R. (1992). A search for intact lava tubes on the Moon: Possible lunar base habitats. In W. W. Mendell (Ed.), *The Second Conference on Lunar Bases and Space Activities of the 21st Century*, NASA Conferences Publication 3166, 1 (Parts 1–4) & 2 (Parts 5–8) (pp. 219–229).

Elston, D. P., & Willingham, C. R. (1969). Five-day mission plan to investigate the geology of the Marius Hills region of the Moon, (pp. 55). U.S. Geological Survey Open-File Report 69-91.

Greeley, R. (1971). Lava tubes and channels in the lunar Marius Hills. *Moon*, *3*, 289–314. https://doi.org/10.1007/BF00561842

Haruyama, J., Hioki, K., Shirao, M., Morota, T., Hiesinger, H., van der Bogert, C. H., … Pieters, C. M. (2009). Possible lunar lava tube skylight observed by SELENE cameras. *Geophysical Research Letters*, *36*, L21206. https://doi.org/10.1029/2009GL040635

Haruyama, J., Hara, S., Hioki, K., Morota, T., Yokota, Y., Shirao, M., … Paul, G. L. (2010). New discoveries of lunar holes in Mare Tranquilltatis and Mare Ingenii, Lunar Planet. Sci. Conf. 41, Abstract 1285.

Haruyama, J., Morota, T., Kobayashi, S., Sawai, S., Lucey, P. G., Shirao, M., & Nishino, M. N. (2012). Lunar Holes and Lava Tubes as Resources for Lunar Science and Exploration. *Moon*, 139–163. https://doi.org/10.1007/978-3-642-27969-0_6

Haruyama, J., Kawano, I., Kubota, T., Otsuki, M., Kato, H., Nishibori, T., … Michikawa, Y. (2016). Mission concepts of unprecedented Zipangu Underworld of the Moon Exploration (UZUME) Project. *Transactions of the Japan Society for Aeronautical and Space Sciences, Aerospace Technology Japan*, *14*(ists30), 147–150. https://doi.org/10.2322/tastj.14.Pk_147

Hörz, F. (1985). Lava tubes: Potential shelters for habitats. In W. W. Mendell (Ed.), *Lunar Bases and Space Activities of the 21st Century* (A86-30113 13-14) (pp. 405–412). Houston, TX: Lunar and Planet. Inst. https://doi.org/10.1016/0016-7037(87)90018-4

Karlstrom, T. N. V., McCauley, J. F., & Swann, G. A. (1968). Preliminary lunar exploration plan of the Marius Hills region of the Moon, (42 pp.). U.S. Geologocal Survey Open-File Report 68-155.

Kobayashi, T., Kim, J.-H., Lee, S. R., Kumamoto, A., Nakagawa, H., Oshigami, S., … Ono, T. (2012). Synthetic aperture radar processing of Kaguya Lunar Radar Sounder Data for lunar subsurface imaging. *IEEE Transactions on Geoscience and Remote Sensing*, *50*, 2161–2174. https://doi.org/10.1109/TGRS.2011.2171349

Miyamoto, H., Haruyama, J.'i., Kobayashi, T., Suzuki, K., Okada, T., Nishibori, T., … Masumoto, K. (2005). Mapping the structure and depth of lava tubes using ground penetrating radar. *Geophysical Research Letters*, *32*, L21316. https://doi.org/10.1029/2005GL024159

Oberbeck, V. R., Quaide, W. L., & Greeley, R. (1969). On the origin of lunar sinuous rilles. *Modern Geologist*, *1*, 75–80.

Ono, T., Kumamoto, A., Nakagawa, H., Yamaguchi, Y., Oshigami, S., Yamaji, A., … Oya, H. (2009). Lunar radar sounder observations of subsurface layers under the nearside Maria of the Moon. *Science*, *323*, 909–912. https://doi.org/10.1126/science.1165988

Oshigami, S., Okuno, S., Yamaguchi, Y., Ohtake, M., Haruyama, J., Kobayashi, T., … Onod, T. (2012). The layered structure of lunar Maria: Identification of the HF-radar reflector in Mare Serenitatis using multiband optical images. *Icarus*, *218*, 506–512. https://doi.org/10.1016/j.icarus.2011.12.026

Oshigami, S., Watanabe, S., Yamaguchi, Y., Yamaji, A., Kobayashi, T., Kumamoto, A., … Ono, T. (2014). Mare volcanism: Reinterpretation based on Kaguya Lunar Radar Sounder data. *Geophysical Research Letters*, *119*, 1037–1045. https://doi.org/10.1002/2013JE004568

Phillips, R. J., Adams, G. F., Brown, W. E., Jr., Eggleton, R. E., Jackson, P., Jordan, R., … Zelenka, J. S. (1973). Apollo Lunar Sounder Experiment, NASA Special Publication 330, 22-1-22-26.

Robinson, M. S., Ashley, J. W., Boyd, A. K., Wagner, R. V., Speyerer, E. J., Ray Hawke, B., … Van Der Bogert, C. H. (2012). Confirmation of sublunarean voids and thin layering in mare deposits. *Planetary and Space Science*, *69*, 18–27. https://doi.org/10.1016/j.pss.2012.05.008

Seu, R., Phillips, R. J., Alberti, G., Biccari, D., Bonaventure, F., Bortone, M., … Vicari, D. (2007). Accumulation and erosion of Mars' south polar layered deposits. *Science*, *317*, 1715–1718, https://doi.10.1126/science.1144129

Seu, R., Biccari, D., Orosei, R., Lorenzoni, L. V., Phillips, R. J., Marinangenli, L., … Zampolini, E. (2004) SHARAD: The MRO 2005 shallow radar. *Planetary and Space Science*, *52*, 157–166. https://doi.10.1016/j.pss.2003.08024

Thurber, C. H., & Solomon, S. C. (1978). An assessment of crustal thickness variations on the lunar nearside: Models, uncertainties, and implications for crustal differentiation, Proc. Lunar Planet. Sci. Conf., 9th, 3481–3497.

Wagner, R. V., & Robinson, M. S. (2014). Distribution, formation mechanisms, and significance of lunar pits. *Icarus*, *237*, 52–60. https://doi.org/10.1016/j.icarous.2014.04.002

Yamamoto, K., Haruyama, J., Kobayashi, S., Ohtake, M., Iwata, T., Ishihara, Y., & Hasebe, N. (2016). Two-stage development of the lunar farside highlands crustal formation. *Planetary and Space Science*, *120*, 43–47. https://doi.org/10.1016/j.pss.2015.11.002

Zuber, M., Smith, D. E., Lehman, D. H., Hoffman, T. L., Asmar, S. W., & Watkins, M. M. (2013). Gravity Recovery and Interior Laboratory (GRAIL): Mapping the lunar interior from crust to core. *Space Science Reviews*, *178*, 3–24. https://doi.org/10.1007/s11214-012-9952-7

Zuber, M., Smith, D. E., Watkins, M. M., Asmar, S. W., Konopliv, A. S., Lemoine, F. G., … Yuan, D. N. (2013). Gravity field of the Moon from the Gravity Recovery and Interior Laboratory (GRAIL) mission. *Science*, *339*, 668–671. https://doi.org/10.1126/science.1231507